Biogeosciences Discuss., 9, 2153–2168, 2012
www.biogeosciences-discuss.net/9/2153/2012/
doi:10.5194/bgd-9-2153-2012

Biogeosciences Discussions

Direct observations of diel biological CO_2 fixation in the oceans

H. Thomas[1], S. E. Craig[1], B. J. W. Greenan[2], W. Burt[1], G. J. Herndl[3,4], S. Higginson[1], L. Salt[4], E. H. Shadwick[1,5], and J. Urrego-Blanco[1]

[1]Dalhousie University, Department of Oceanography, Halifax, NS, Canada
[2]Bedford Institute of Oceanography, Fisheries and Oceans Canada, Dartmouth, NS, Canada
[3]University of Vienna, Department of Marine Biology, Vienna, Austria
[4]Royal Netherlands Institute for Sea Research, Department of Biological Oceanography, Texel, The Netherlands
[5]Antarctic Climate and Ecosystems Cooperative Research Centre, University of Tasmania, Hobart, Tasmania, Australia

Received: 10 February 2012 – Accepted: 13 February 2012 – Published: 24 February 2012

Correspondence to: H. Thomas (helmuth.thomas@dal.ca)

Published by Copernicus Publications on behalf of the European Geosciences Union.

Abstract

Much of the variability in the surface ocean's carbon cycle can be attributed to the availability of sunlight, through processes such as heat fluxes and photosynthesis, which regulate over a wide range of time scales. The critical processes occurring on timescales of a day or less, however, have undergone few investigations, and most of these have been limited to a time span of several days to months, or exceptionally, for longer periods. Optical methods have helped to infer short-term biological variability, however corresponding investigations of the oceanic CO_2 system are lacking. We employ high-frequency CO_2 and optical observations covering the full seasonal cycle on the Scotian Shelf, Northwestern Atlantic Ocean, in order to unravel diel periodicity of the surface ocean carbon cycle and its effects on annual budgets. Significant diel periodicity occurs only if the water column is sufficiently stable as observed during seasonal warming. During that time biological CO_2 drawdown, or net community production (NCP), is delayed for several hours relative to the onset of photosynthetically available radiation (PAR), due to diel cycles in chlorophyll-*a* concentration and to grazing, both of which, we suggest, inhibit NCP in the early morning hours. In summer, NCP decreases by more than 90 %, coinciding with the seasonal minimum of the mixed layer depth and resulting in the disappearance of the diel CO_2 periodicity in the surface waters.

1 Introduction

Shelf and marginal seas play a crucial role in the global carbon cycle as they link its different compartments (land, ocean, atmosphere) (Ciais et al., 2008; Thomas et al., 2008; Chen and Borges, 2009). As a consequence of their role as an integral link between the compartments, the spatial and temporal variability of the carbon cycle in marginal seas is generally higher than in open ocean environments (Thomas and Schneider, 1999; Schiettecatte, 2006; Chen and Borges, 2009; Omar et al., 2010). In

BGD
9, 2153–2168, 2012

addition to natural drivers, anthropogenic processes perturbing natural cycles in each of the carbon cycle compartments affect variability in shelf and marginal seas. Examples of such perturbations include eutrophication, ocean acidification and atmospheric nitrogen deposition (Doney et al., 2007; Thomas et al., 2009; Borges and Gypens, 2010; Cai et al., 2011).

Physical, biological and chemical processes govern the variability of the carbon cycle and the air-sea exchange of CO_2. Although these processes are evident at many temporal and spatial scales, they interact at high frequency, local scales, eventually yielding diurnal, seasonal and longer-term periodicity. Our understanding of the monthly to seasonal variability in the carbon cycle in several shelf and marginal seas has improved, in particular with respect to attaining full annual observational coverage (Chen and Borges, 2009; Omar et al., 2010; Thomas et al., 2004; Shadwick et al., 2010, 2011). At shorter time scales, optical methods have helped to infer short-term biological variability (Siegel et al., 1989; Stramska and Dickey, 1992; Cullen et al., 1992; Gernez et al., 2011; Dall'Olmo et al., 2011), however corresponding investigations of the oceanic CO_2 system are largely lacking. Only a few recent studies have mainly focused on time scales of several days to months (Hood et al., 2001; Bates et al., 2001; Copin-Montegut et al., 2004; Lefevre et al., 2008; Bozec et al., 2011), and investigations of processes at the rate of their occurrence in shelf and marginal seas are still sparse when it comes to full seasonal coverage (Vandemark et al., 2011).

The Scotian Shelf region is located at the Eastern Canadian continental shelf at the boundary between the subpolar and subtropical gyres. This region is thus influenced by water masses of arctic origin via the Labrador and Newfoundland Shelves, by low-salinity waters emanating from the Gulf of St. Lawrence, and by the Gulf Stream (Urrego-Blanco and Sheng, 2012). One of the dominant characteristics on the shelf is the large seasonal amplitude in sea surface temperature (SST) between subzero temperatures in winter to approximately 20 °C during summer (Shadwick and Thomas, 2011) (Fig. 1). Recent studies have identified the region as a strong source for atmospheric CO_2 at the annual scale, with an intense, but brief period of CO_2 uptake during

BGD
9, 2153–2168, 2012

the spring bloom, which occurs at the annual SST minimum in late March to early April (Shadwick et al., 2011) (Fig. 1). Controls of the seasonal to interannual variability of the surface CO_2 system in the Scotian Shelf region have been inferred from satellite observations, and include the intensity of autumn and winter storms, winter nutrient levels, and the onset of post-winter water column stratification (Greenan et al., 2004, 2008; Shadwick et al., 2010). The processes controlling the variability of the carbon cycle at time scales shorter than the monthly to seasonal scale remain poorly understood, which is the case for most regions of the open oceans, as well as shelf and marginal seas. The study, presented here, sheds light on the role of high frequency processes in controlling the carbon cycle in the surface waters of the Scotian Shelf region over a complete annual cycle.

2 Material and methods

We employ observations from a CARIOCA buoy recording surface water pCO_2, SST, salinity, and complementary parameters at an hourly rate. The buoy has been deployed since April 2007. In order to avoid data gaps due to maintenance, we reconstruct an annual cycle using different years of observations. Detailed descriptions of the buoy location and the corresponding sampling activities have been given in Shadwick et al. (2011). In the present study, we focus on three key periods of the annual cycle: 1: winter (pre-spring bloom to spring bloom transition); 2: late spring to early summer, i.e., the warming period; and 3: the autumn to winter transition (Fig. 1). Diel cycles in pCO_2 with hourly resolution were established by removing the 48-point moving average from the (hourly) observations. In order to investigate the crucial period between spring and summer, when the waters are warming (Fig. 1), we combined the CARIOCA data with observations from the SeaHorse, an autonomous profiler (Greenan et al., 2004, 2008), which records water column profiles of temperature, salinity, photosynthetically available radiation (PAR), and downwelling irradiance ($E_d(\lambda)$). Profiles were recorded with approximately 0.5 m vertical resolution approximately every 2 h between 4 April and 27

BGD
9, 2153–2168, 2012

July 2007. In an attempt to resolve the contribution of phytoplankton to NCP during the warming period, we derived chlorophyll-*a* concentration from profiles of Seahorse $E_d(\lambda)$ using the model of Nahorniak et al. (2001). This required calculation of the attenuation of E_d at three wavelengths over a depth interval (5–6 m) that was similar to the depths at which other CARIOCA parameters were measured. Since the sensor wavelengths did not exactly match the wavelengths required by the model, $E_d(\lambda)$ was interpolated to model wavelengths (412, 443, 555 nm). Modelled chlorophyll-*a* (Chl_{mod}; $mg\,m^{-3}$) was then calculated using Nahorniak et al. (2001) formulations that include spectral coefficients to describe the absorption properties of water, phytoplankton and coloured dissolved organic matter and assume a value of 0.8 for the average cosine of downwelling light, μ_d (dimensionless). Chl_{mod} values were compared with discrete, fluorometrically determined chlorophyll-*a* values obtained at the same time and depth from ship-based water samples; R^2 and root mean square error (RMSE) values of 0.89 and 0.83 $mg\,m^{-3}$ ($N = 8$), respectively, were obtained. These values were then averaged into time bins over the 40-day period to give climatological values for Chl_{mod} every two hours during the hours of daylight during which reliable $E_d(\lambda)$ measurements could be made, which, at this time of year and latitude, corresponded to times between ~ 06:00h–16:00 LT.

3 Results and discussion

The spectral analysis of the buoy data (Fig. 2a,b) revealed a 24-h periodicity for the parameters pCO_2 and SST that occurs only when the waters are warming, i.e., between April and late August. pCO_2 and SST also show significant coherent patterns during this time of the year (Fig. 2b, bottom panel) and are the focus of this paper. Outside of this period, periodicity and significant coherence were only observed, if detectable, at longer time scales (several days), which mirrors the typical frequency of winter storms in the region (Fig. 2c). Other parameters such as salinity do not show significant 24-h periodicity, which means that tidal, lateral and other effects are either not identifiable, or

BGD
9, 2153–2168, 2012

act on timescales longer than 24 h. Such processes would be captured by the 48-point moving average, and do not influence the diel cycles.

Surface heat fluxes cause variability in SST at diel and seasonal time scales (Umoh and Thompson, 1994), which in turn drive some of the observed variability of the pCO_2, primarily because of the temperature dependence of the Henry constant. We corrected the observed pCO_2 data ($pCO_{2,obs}$) to a daily mean temperature to give $pCO_{2,temp}$. The difference between $pCO_{2,obs}$ and $pCO_{2,temp}$ yielded pCO_2 data that are governed by processes other than temperature within a 24-h period. Since we did not detect processes other than SST variability acting on the 24 h period, the remaining pCO_2 variability can be ascribed to biological activity ($pCO_{2,bio}$). The daily and diel variability of the $pCO_{2,obs}$ and $pCO_{2,bio}$ for three periods of the year is shown in Fig. 3. In the winter period (days 80–95, Fig. 3a), the amplitude of the diel oscillation was small and the pCO_2 relatively constant. With the onset of the spring bloom, at approximately day 90, the diel amplitude drastically increased (Fig. 3a). Throughout both of these periods, $pCO_{2,obs}$ and $pCO_{2,bio}$ were in phase and tracked each other closely indicating that temperature was not the main driver for the short-term variability during this time of the year. Similarly, in the autumn to winter (Fig. 3b) transition $pCO_{2,obs}$ and $pCO_{2,bio}$ again revealed in-phase patterns, though with a higher amplitude in autumn (days 305–345) than in winter (days 80–95), which can be ascribed to deepening of the mixed layer and an intrusion of high pCO_2 subsurface waters into the surface mixed layer (Shadwick et al., 2011). Between the days 160–200 (end of June until end of July), i.e., later in the season of surface water warming, the amplitude of the diel oscillation was reduced compared to that observed during the spring bloom (Fig. 3a–c). More importantly, a phase shift was detectable between $pCO_{2,obs}$ and $pCO_{2,bio}$, with the latter occuring approximately 3 h earlier than the $pCO_{2,obs}$ (Fig. 3d). We postulate that the cause for this phase shift might be diel cycles in biological activity. Such diel cycles were only visible, when the water column was sufficiently stable such as during thermal stratification (Fig. 1b; Shadwick et al. (2011), their Fig. 9).

BGD
9, 2153–2168, 2012

We can consider the diel cycle of pCO_2 as a composite of a temperature driven component, which follows the diel cycle of SST (Fig. 3d), and a biologically driven component, controlled by the balance of production and respiration of organic matter. The diel biological cycle obtained here can be considered a net biological signal, which shows an increase of the $pCO_{2,bio}$, i.e., net respiration, beginning in the evening (approx. 21:00 h), and ending in the morning hours (10:00h–11:00 h), when net community production (NCP) begins to exceed community respiration. NCP, indicated by a negative gradient in the pCO_2 anomaly (Fig. 3d), dominates the system until dusk. Subtracting the respiration signal, computed from the slope of the $pCO_{2,bio}$ during nighttime conditions, allows us to estimate the diurnal cycle of gross primary production (GPP). The corresponding respiration rate, assumed to be constant throughout the day, is estimated to be 0.05 µmol C $(l\,h)^{-1}$; the rates of NCP and GPP are 0.26 µmol C $(l\,h)^{-1}$ and 0.31 µmol C $(l\,h)^{-1}$, respectively, both lasting approximately 10 h per day.

The onset of the net photosynthetic CO_2 drawdown occurs approximately 4–5 h after sunrise, near the period maximum of PAR (Fig. 3d) – a phenomenon that has been documented frequently but surprisingly, has rarely been discussed or addressed in detail. Stramska and Dickey (1992), Siegel et al. (1989) or Gernez et al. (2011) report a phase shift of several hours between the onset of PAR and maximum values of either the beam attenuation coefficient (c_p) or dissolved oxygen (O_2) concentrations, the latter two mirroring the build up of photosynthetic organic matter and revealing phasing throughout the diurnal cycle, which is comparable to the phasing of $pCO_{2,bio}$. Bozec et al. (2011, their Fig. 5) also show a similar phase shift between dissolved O_2 and pCO_2, relative to PAR, however, these authors conclude that pCO_2 and PAR are out of phase by 180 degrees and O_2 is in phase with PAR. In summary, it appears that there is sufficient evidence in the literature to suggest that the signal of net biological carbon fixation in the water column, as revealed by pCO_2, O_2 or beam attenuation measurements, is detectable at or around peak PAR, which is the ultimate energy source for the biological carbon fixation.

BGD
9, 2153–2168, 2012

In order to determine whether this reported periodicity in metrics of phytoplankton photosynthetic activity occurred at our study site, we used the model of Nahorniak et al. (2001) to derive estimates of chlorophyll-*a* concentration (Chl_{mod}; mg m^{-3}) every two hours during daylight from SeaHorse profiler measurements of multispectral downwelling irradiance, $E_d(\lambda)$. When averaged over the day 160–200 period, a diel cycle in Chl_{mod} was revealed with a difference of ∼30 % between minimum and maximum values, and where the lowest values corresponded to low PAR levels during early morning and late afternoon, and maximum values to peak PAR at ∼midday (Fig. 3d). When compared with the pCO_2 diel cycles, it was observed that onset of net CO_2 drawdown, indicated by the change in gradient of $pCO_{2,bio}$ from positive to negative, coincided with the time of the maximum Chl_{mod} values. In other words, our data suggest that a threshold Chl_{mod} must first be attained before the system achieves net CO_2 drawdown. Others have also reported diel signals in either Chl-*a* or photosynthetic parameters (Cullen et al., 1992; Bruyant et al., 2005), with peak values around midday. It should also be noted that photoinhibition may depress photosynthetic rate at high irradiances, especially near midday, potentially further modulating the exact occurrence of net CO_2 drawdown with respect to PAR levels.

Both our results and those reported in the literature are consistent with the notion of a phase shift between the onset of PAR at daybreak and of net carbon fixation at approximate solar noon. Meso- and microzooplankton, which are active during nighttime, might still exert grazing pressure on phytoplankton during the early morning hours and thereby keep the abundance of phytoplankton low during the initial hours of daylight (Siegel et al., 1989). In addition to grazing effects, the diurnal variability in phytoplankton photosynthetic activity itself also contributes to delaying net carbon fixation until PAR has reached approximately maximum values as discussed above. Furthermore, in order to detect net carbon fixation as a change in the pCO_2 and O_2 concentrations in the water column, primary producers have to compensate for the respiratory activity of the heterotrophs, which in turn might exhibit relatively constant activity rates throughout the diel cycle (Cullen et al., 1992; Gernez et al., 2011). Based on our analysis,

BGD
9, 2153–2168, 2012

we suggest that grazing and the dependence of the photosynthetic rate on PAR would cause the ecosystem to become autotrophic just before or at maximum PAR values (Fig. 3d). In our study, we were not able to identify any diurnal variability in the water column structure, i.e., in strength and depth of stratification, which might have provoked the phase shift between PAR and $pCO_{2,bio}$.

We have obtained the seasonal dynamics of NCP integrating the hourly $pCO_{2,bio}$ values (Fig. 4.). The maximum value of NCP is 3.4 mol C m^{-2}, or 271 µmol C l^{-1}. Of particular interest is the observation that the carbon fixation rate, i.e., the DIC uptake rate by phytoplankton, is fairly constant from the onset of the spring bloom (approx. day 100) to approximately day 180, with DIC uptake rates of approximately 2.5 µmol C $(l\,d)^{-1}$, corresponding to a NCP rate of 0.26 µmol C $(l\,h)^{-1}$, assuming a 10-h photoperiod per day (Fig. 3d). The production rate decreases to about 0.1 µmol C $(l\,d)^{-1}$ (Fig. 4), when the mixed layer depth reaches its minimum. Thereafter, a combination of dramatically reduced availability of nutrients and light inhibition make NCP almost vanish.

4 Conclusions

In summary, we observed a statistically significant diurnal periodicity of the CO_2 system only during the period, when the water is warming. The corresponding increase in water column stability facilitates the appearance of the diurnal cycle. The unraveled diurnal cycles of the surface pCO_2 reveal that net photosynthetic carbon fixation, i.e., NCP, begins approximately 4–5 h after onset of PAR. Grazing and transitional metabolic rates are likely the responsible processes for this phase shift, eventually allowing the ecosystem to be autotrophic for approximately 10 h out of 16 h of daylight.

Acknowledgements. We gratefully acknowledge support from the Canadian Foundation for Climate and Atmospheric Sciences (CFCAS), the National Science and Engineering Research Council (NSERC), Metocean Datasystems, as well as the BIO Technical Operations Group. HT holds a Canada Research Chair for Marine Biogeochemistry. This work is a contribution to the IGBP/IHDP core project LOICZ.

BGD
9, 2153–2168, 2012

References

Bates, N. R., Samuels, L., and Merlivat, L.: Biogeochemical and physical factors influencing seawater fCO_2 and air-sea CO_2 exchange on the Bermuda coral reef, Limnol. Oceanogr., 46(4), 833–846, 2001.

Borges, A. V. and Gypens, N.: Carbonate chemistry in the coastal zone responds more strongly to eutrophication than to ocean acidification, Limnol. Oceanogr., 55, 346–353, 2010.

Bozec, Y., Merlivat, L., Baudoux, A.-C., Beaumont, L., Blain, S., Bucciarelli, E., Danguy, T., Grossteffan, E., Guillot, A., Guillou, J., Répécaud, M., and Tréguer, P.: Diurnal to inter-annual dynamics of pCO_2 recorded by a CARIOCA sensor in a temperate coastal ecosystem (2003–2009), Mar. Chem., 126, 13–26, 2011.

Bruyant, F., Babin, M., Genty, B., Prasil, O., Behrenfeld, M. J., Claustre, H., Bricaud, A., Garczarek, L., Holtzendorff, J., Koblizek, M., Dousova, H., and Partensky, F.: Diel variations in the photosynthetic parameters of *Prochlorococcus* strain PCC 9511: combined effects of light and cell cycle, Limnol. Oceanogr., 56, 850–863, 2005.

Cai, W.-J., Hu, X., Huang, W.-J., Murrell, M. C., Lehrter, J. C., Lohrenz, S. E., Chou, W.-C., Zhai, W., Hollibaugh, J. T., Wang, Y., Zhao, P., Guo, X., Gundersen, K., Dai, M., and Gong, G.-C.: Acidification of subsurface coastal waters enhanced by eutrophication, Nat. Geosci., 4, 766–770, 2011.

Chen, C.-T. A. and Borges, A. V.: Reconciling opposing views on carbon cycling in the coastal ocean: continental shelves as sinks and near-shore ecosystems as sources of atmospheric CO_2, Deep-Sea Res. II, 56, 578–590, 2009.

Ciais, P., Borges, A. V., Abril, G., Meybeck, M., Folberth, G., Hauglustaine, D., and Janssens, I. A.: The impact of lateral carbon fluxes on the European carbon balance, Biogeosciences, 5, 1259–1271, doi:10.5194/bg-5-1259-2008, 2008.

Copin-Montegut, C., Begovic, M., and Merlivat, L.: Variability of the partial pressure of CO_2 on diel to annual time scales in the Northwestern Mediterranean Sea, Mar. Chem., 85, 169–189, 2004.

Cullen, J. J., Lewis, M., Davis, C. O., and Barber, R.: Photosynthetic characteristics and estimated growth rates indicate grazing is the proximate control of primary production in the Equatorial Pacific, J. Geophys. Res., 97, 639–655, 1992.

Dall'Olmo, G., Boss, E., Behrenfeld, M. J., Westberry, T. K., Courties, C., Prieur, L., Pujo-Pay, M., Hardman-Mountford, N., and Moutin, T.: Inferring phytoplankton carbon and eco-

BGD
9, 2153–2168, 2012

physiological rates from diel cycles of spectral particulate beam-attenuation coefficient, Biogeosciences, 8, 3423–3439, doi:10.5194/bg-8-3423-2011, 2011.
Doney, S. C., Mahowald, N., Lima, I., Feely, R. A., Mackenzie, F. T., Lamarque, J.-F., and Rasch, P. J.: Impact of anthropogenic atmospheric nitrogen and sulphur deposition on ocean acidification and the inorganic carbon system, P. Natl. Acad. Sci., 104, 14580–14585, 2007.
Gernez, P., Antoine, D., and Huot, Y.: Diel cycles of the particulate beam attenuation coefficient under varying trophic conditions in the Northwestern Mediterranean Sea: observations and modeling, Limnol. Oceanogr., 56, 17–36, 2011.
Greenan, B. J. W., Petrie, B. D., Harrison, W. G., and Oakey, N. S.: Are the spring and fall blooms on the Scotian Shelf related to short-term physical events?, Cont. Shelf Res., 24, 603–625, 2004.
Greenan, B. J. W., Petrie, B. D., Harrison, W. G., and Strain, P. M.: The onset and evolution of a spring bloom on the Scotian Shelf, Limnol. Oceanogr., 53, 1759–1775, 2008.
Hood, E. M., Wanninkhof, R., and Merlivat, L.: Short timescale variations of fCO_2 in a North Atlantic warm-core eddy: results from the Gas-Ex 98 carbon interface ocean atmosphere (CARIOCA) buoy data, J. Geophys Res., 106, 2561–2575, 2001.
Lefevre, N., Guillot, A., Beaumont, L., and Danguy, T.: Variability of fCO_2 in the Eastern Tropical Atlantic from a moored buoy, J. Geophys. Res., 113, C01015, 2008.
Nahorniak, J. S., Abbott, M. R., Letelier, R. M., and Pegau, W. S. C.: Analysis of a method to estimate chlorophyll-*a* concentration from irradiance measurements at varying depths, J. Atmos. Ocean. Technol., 18, 2063–2073, 2001.
Omar, A. M., Olsen, A., Johannessen, T., Hoppema, M., Thomas, H., and Borges, A. V.: Spatiotemporal variations of fCO_2 in the North Sea, Ocean Sci., 6, 77–89, doi:10.5194/os-6-77-2010, 2010.
Schiettecatte, L.-S., Gazeau, F., van der Zee, C., Brion, N., and Borges, A. V.: Time series of the partial pressure of carbon dioxide (2001–2004) and preliminary inorganic carbon budget in the Scheldt plume (Belgian coast waters), Geochem. Geophys. Geosys., 7, Q06009, doi:10.1029/2005GC001161, 2006.
Shadwick, E. H. and Thomas, H.: Carbon dioxide in the coastal ocean: a case study in the Scotian Shelf region, in: Ocean Year Book, 25, edited by: Chircop, A., Coffen-Smout, S., and McConnell, M., Martinus Nijhoff, Leiden/Boston, 171–204, 2011.
Shadwick, E. H., Thomas, H., Comeau, A., Craig, S. E., Hunt, C. W., and Salisbury, J. E.: Air-Sea CO_2 fluxes on the Scotian Shelf: seasonal to multi-annual variability, Biogeosciences,

BGD
9, 2153–2168, 2012

7, 3851–3867, doi:10.5194/bg-7-3851-2010, 2010.
Shadwick, E. H., Thomas, H., Azetsu-Scott, K., Greenan, B. J. W., Head, E., and Horne, E.: Seasonal variability of dissolved inorganic carbon and surface water pCO_2 in the Scotian Shelf region of the Northwestern Atlantic, Mar. Chem., 124, 23–37, 2011.
Siegel, D. A., Dickey, T. D., Washburn, L., Hamilton, M. K., and Mitchell, B. G.: Optical determination of particulate abundance and production variations in the oligotrophic ocean, Deep-Sea Res. I, 36, 211–222, 1989.
Stramska, M. and Dickey, T. D.: Variability of bio-optical properties of the upper ocean associated with diel cycles in phytoplankton population, J. Geophys. Res., 97, 17873–17887, 1992.
Thomas, H. and Schneider, B.: The seasonal cycle of carbon dioxide in Baltic Sea surface waters, J. Mar. Sys., 22, 53–67, 1999.
Thomas, H., Bozec, Y., Elkalay, K., and de Baar, H. J. W.: Enhanced open ocean storage of CO_2 from shelf sea pumping, Science, 304(5673), 1005–1008, 2004.
Thomas, H., Unger, D., Zhang, J., Liu, K.-K., and Shadwick, E. H.: Biogeochemical cycling in semi-enclosed marine systems and continental margins, in: Watersheds, Bays and Bounded Seas (SCOPE No. 70), edited by: Urban, E., Sundby, B., Malanotte-Rizzoli, P., and Melillo, J., Island Press, Washington, DC, 169–190, 2008
Thomas, H., Schiettecatte, L.-S., Suykens, K., Koné, Y. J. M., Shadwick, E. H., Prowe, A. E. F., Bozec, Y., de Baar, H. J. W., and Borges, A. V.: Enhanced ocean carbon storage from anaerobic alkalinity generation in coastal sediments, Biogeosciences, 6, 267–274, doi:10.5194/bg-6-267-2009, 2009.
Umoh, J. U. and Thompson, K. R.: Surface heat flux, horizontal advection, and the seasonal evolution of water temperature on the Scotian Shelf, J. Geophys. Res., 99, 403–420, 1994.
Urrego-Blanco, J. and Sheng, J.: Interannual variability of circulation and hydrography over the Eastern Canadian Continental Shelf, Atmosphere-Ocean, in press, 2012.
Vandemark, D., Salisbury, J. E., Hunt, C. W., Shellito, S., and Irish, J.: Temporal and spatial dynamics of CO_2 air-sea flux in the Gulf of Maine, J. Geophys. Res., 116, C01012, doi:10.1029/2010JC006408, 2011.

BGD
9, 2153–2168, 2012

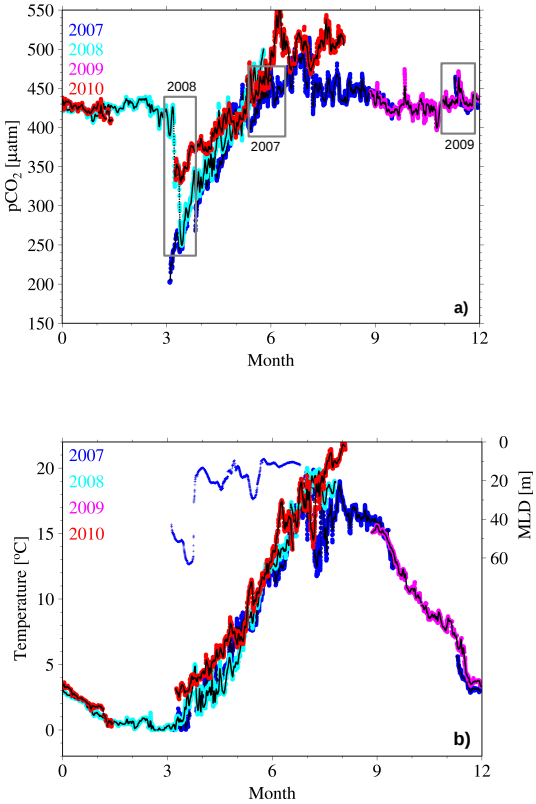

Fig. 1. Composite of available pCO_2 **(a)** and temperature data **(b)** for the years 2007–2010, recorded by the CARIOCA buoy. For the further study we evaluate data from June/July 2007, April 2008 and November/December 2009 as indicated by the gray boxes in a), assuming a climatological annual cycle. The black lines indicate the 48-point moving average. In **(b)**, the depth of the maximum of the Brunt-Väisälä frequency is shown as measure of the mixed layer depth (MLD), computed from the Seahorse data, deployed between April 2007 and July 2007.

BGD
9, 2153–2168, 2012

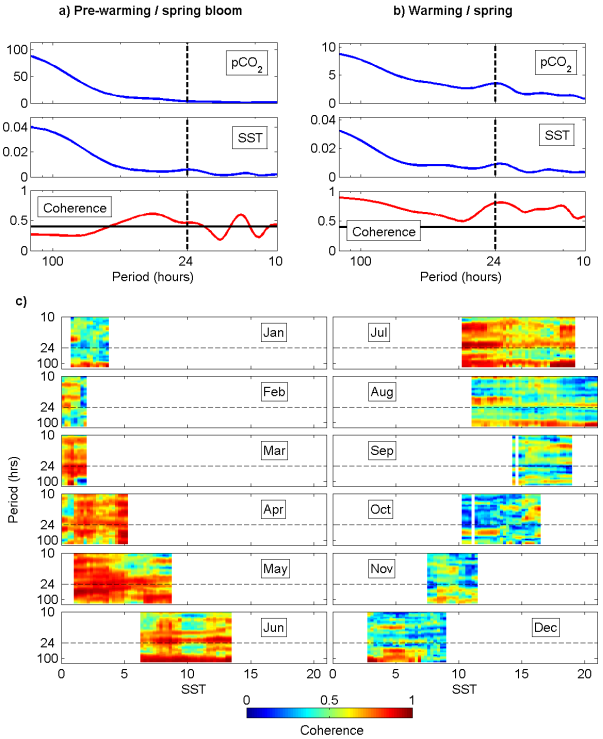

Fig. 2. Spectral analysis of pCO_2 and SST data from the CARIOCA buoy. Power spectra of pCO_2 and SST and their coherence are shown for two periods: **(a)** the pre-warming/spring bloom period and **(b)** the warming period (see Fig. 1a gray boxes). The dashed line on each plot indicates the 24 h period, and the horizontal solid line on the coherence plots shows the 5 % significance level based on the degrees of freedom of the cross-spectral estimators. The coherence between pCO_2 and SST is plotted as a function of SST in monthly composites **(c)**, illustrating the temporal evolution of the coherence. The color scale indicates the level of coherence between pCO_2 and SST, and the dashed line shows the 24 h period. High coherence at the 24 h period occurs only during the period when the water is warming.

BGD
9, 2153–2168, 2012

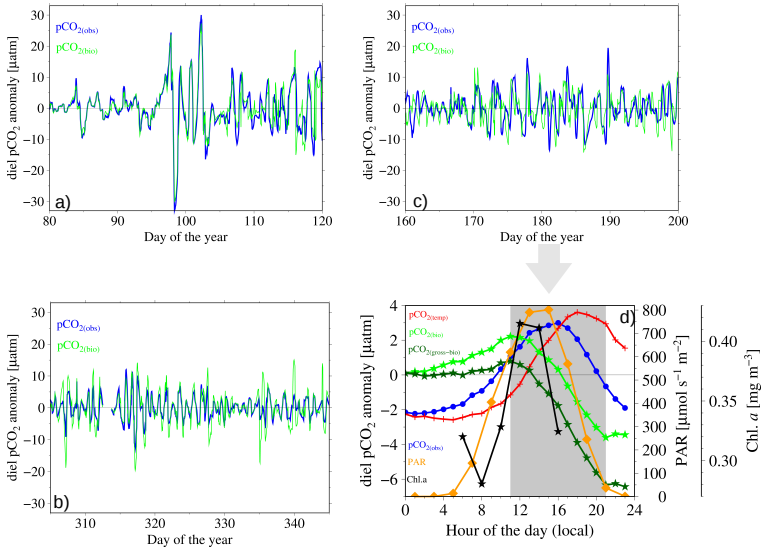

Fig. 3. Diel anomalies and daily cycles of observed pCO_2, biologically controlled pCO_2, PAR, and Chl-*a*. We show diel anomalies of $pCO_{2,obs}$ (blue) and $pCO_{2,bio}$ (green) for three periods of the year **(a–c)** as depicted in Fig. 1. Note the phase shift in the warming period **(c,d)**, while outside the warming period **(a,b)** both parameters show the same timing (i.e., they are independent). Average diel anomalies or daily cycles compiled for the 40-day period from days 160–200 (see Fig. 1) observed pCO_2 ($pCO_{2,obs}$, blue), biologically controlled pCO_2 ($pCO_{2,bio}$, green), temperature-only controlled pCO_2 ($pCO_{2,temp}$, red), $pCO_{2,bio}$ corrected for respiratory activity ($pCO_{2,gross\text{-}bio}$, dark green) and photosynthetic active radiation (PAR, orange). Chlorophyll-*a* (chl-*a*, black) is shown for the hours (6.00 h–16.00 h), when reliable $E_d(\lambda)$ measurements can be made by the Seahorse. The gray-shaded box indicated the period, when net carbon fixation occurs. Note that $pCO_{2,temp}$ reflects the daily cycle of temperature. The respiration rate has been computed from the slope of the $pCO_{2,bio}$ during night time conditions. The production rates have been computed from the slopes of $pCO_{2,bio}$ and $pCO_{2,gross\text{-}bio}$ during daytime (gray-shaded area), respectively. The time scale reveals local time, i.e., GMT −3 h.

BGD
9, 2153–2168, 2012

Direct observations of diel biological CO_2 fixation in the oceans

H. Thomas et al.

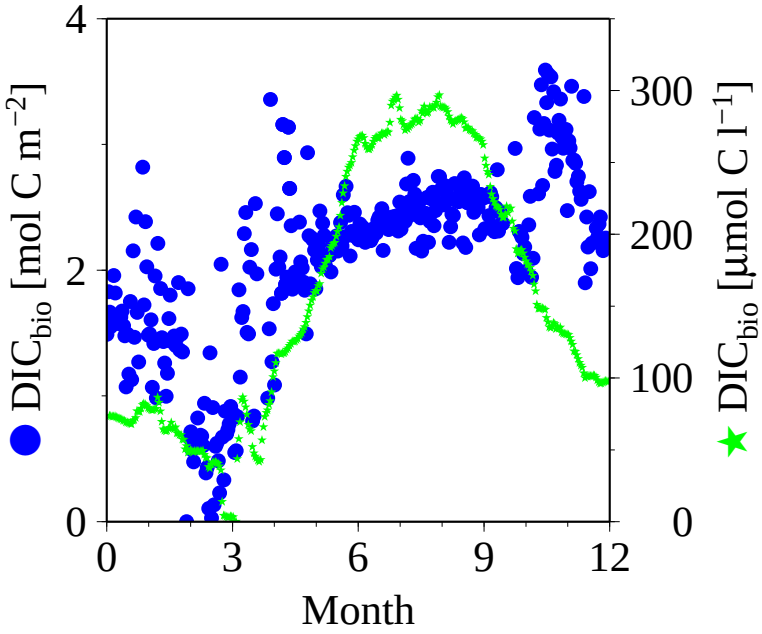

Fig. 4. Annual cycle of biological DIC uptake. We show the annual cycle of biological DIC uptake, integrated from hourly values, shown as mixed layer inventory (left y-axis, blue) and as concentration change (right y-axis, green). The production rate has been computed from the slope of the DIC uptake.

BGD
9, 2153–2168, 2012